THE DIFFERENCE OF BREAKING THROUGH BARRIERS WITH BRILLIANCE

ENABLING GREATER EXPERIMENTAL POWER WITH AN EXTENSIVE PORTFOLIO OF TRUSTED REAGENTS. Every day, researchers at the forefront of discovery trust reagents to power deeper cellular analysis. That's why we deliver innovative dyes to give you more resolution and flexibility in your experimental design. With one of the largest portfolios of high-quality reagents in the industry—backed by scientific publications and unparalleled support—our cutting-edge reagents will help take your research to the next level. **Discover the new BD.**

Learn how you can advance your research >

BD

STEM CELLS®

STEM CELL TECHNOLOGY: EPIGENETICS, GENOMICS, PROTEOMICS AND METABONOMICS

High-Throughput Differentiation and Screening of a Library of Mutant Stem Cell Clones Defines New Host-Based Genes Involved in Rabies Virus Infection

DEEANN WALLIS,[a] KIMBERLY LOESCH,[a] STACY GALAVIZ,[a] QINGAN SUN,[a] MICHAEL DEJESUS,[b] THOMAS IOERGER,[b] JAMES C. SACCHETTINI[a]

Key Words. Embryonic stem cells • Neuronal differentiation • Host-target identification • Genome-wide

[a]Department of Biochemistry and Biophysics and [b]Department of Computer Science and Engineering, Texas A&M University, College Station, Texas, USA

Correspondence: Deeann Wallis, Ph.D., Department of Biochemistry and Biophysics, Interdisciplinary Life Sciences Building Rm 2146B, Texas A&M University, College Station, Texas 77843-3474, USA. Telephone: 979-458-5459; Fax: 979-862-7638; e-mail: dwallis@tamu.edu

Received October 28, 2014; accepted for publication February 2, 2015; first published online in STEM CELLS *EXPRESS* March 5, 2015.

1066-5099/2014/$30.00/0

http://dx.doi.org/10.1002/stem.1983

ABSTRACT

We used a genomic library of mutant murine embryonic stem cells (ESCs) and report the methodology required to simultaneously culture, differentiate, and screen more than 3,200 heterozygous mutant clones to identify host-based genes involved in both sensitivity and resistance to rabies virus infection. Established neuronal differentiation protocols were miniaturized such that many clones could be handled simultaneously, and molecular markers were used to show that the resultant cultures were pan-neuronal. Next, we used a green fluorescent protein (GFP) labeled rabies virus to develop, validate, and implement one of the first host-based, high-content, high-throughput screens for rabies virus. Undifferentiated cell and neuron cultures were infected with GFP-rabies and live imaging was used to evaluate GFP intensity at time points corresponding to initial infection/uptake and early and late replication. Furthermore, supernatants were used to evaluate viral shedding potential. After repeated testing, 63 genes involved in either sensitivity or resistance to rabies infection were identified. To further explore hits, we used a completely independent system (siRNA) to show that reduction in target gene expression leads to the observed phenotype. We validated the immune modulatory gene *Unc13d* and the dynein adapter gene *Bbs4* by treating wild-type ESCs and primary neurons with siRNA; treated cultures were resistant to rabies infection/replication. Overall, the potential of such in vitro functional genomics screens in stem cells adds additional value to other libraries of stem cells. This technique is applicable to any bacterial or virus interactome and any cell or tissue types that can be differentiated from ESCs. STEM CELLS *2015;33:2509–2522*

INTRODUCTION

One of the most powerful tools developed for understanding mammalian gene function is the genetically engineered mouse. Indeed, mouse models have revolutionized the study of gene function and their relationship to disease. A mutant murine embryonic stem cell (ESC) line has already been created for virtually every protein coding gene in the mouse genome through either high-throughput gene trapping or targeting [1–3]. While these ESC lines were created through the Mouse Knockout Project for the purpose of developing and phenotyping mice, these ESC libraries can also be used to conduct genome-wide high-throughput in vitro screens to define host genes that are critical for infection. Unlike siRNA or the use of traditional cell lines, the advantages to screening mutant ESCs and libraries include their unlimited capacity for expansion, stability of the mutation, nonmalignant transformation, normal karyotypes, expression of developmental signaling pathways, and capacity to model complex physiological endpoints. In fact, there have been numerous reports of screening wild-type, undifferentiated murine ESCs [4–7]. However, the fact that ESCs are pluripotent is one of the most advantageous characteristics as it means that the cell lines can be differentiated into specific target cell types while still maintaining the mutation(s) of interest. Libraries of mutant ESCs have never been differentiated and screened in vitro for multiple reasons. First, the heterozygous nature inherent to the mutations in mutant libraries makes it questionable whether it is possible to define robust phenotypes. Second, the simultaneous culture and differentiation of hundreds or even thousands of independent clones is a herculean task.

Rabies virus (RABV) kills at least 55,000 people every year. It is a negative strand RNA virus belonging to genus *Lyssavirus* that causes

inflammatory reaction in its host [8]. While RABV is known for its neurotropism, it is able to infect other cell types as well. The RABV genome encodes only five genes and this small coding capacity demands that virus use host cell machinery for many aspects of its life cycle. As host pathways play such a key role for RABV, this provides a good model system to evaluate host-based targets that modulate the susceptibility and resistance to rabies infection. There is a need for new paradigms for screening as known host-based targets for RABV are limited. Focusing on host-based factors involved in viral infection is important because viral targets may mutate quickly and develop resistance. However, the identification of host targets remains challenging and little is known. As summarized in several reviews [8–10], RABV enters the host cell through host-based cell surface receptors including NGFR, NCAM, and CHRNA, among other as yet unidentified receptors. Viral presence is sensed by the host cell via RIG1. RIG1 is able to detect the RABV 5′-pppRNA. Viral detection leads to the stimulation of interferon (INF) pathways. In fact, this innate immune response is the first defense in virtually all cell types upon recognition of viral molecular patterns and is not specific to RABV. As INF plays such a crucial role in preventing most viral infections, RABV has developed specific mechanisms to subvert this process (reviewed in [10]). Specifically, RABV P protein targets at least three host proteins to block INF response. P inhibits the phosphorylation of IRF3, prevents the nuclear localization of STAT1 and STAT2, and binds PML and retains it in the cytoplasm. All these negatively impact INF signaling. Outside of this basic, nonspecific process, only a few other host-based binding partners have been identified. P also binds Dynein LC8 which affects viral transcription [11]. RABV M binds host-based eIF3h and inhibits its role in translation of cellular mRNAs and effectively down regulates the host cell whole protein production system [9]. Finally, G mRNA interacts with PCBP2 to promote transcript stability and may also affect INF signaling [12].

Possible approaches to identify additional host-based factors typically include: transcriptome studies such as microarray or RNA-Seq analysis; proteomics via two-dimensional differential gel electrophoresis and mass spectrometry; searching for binding partners through yeast two-hybrid (Y2H) and other protein-protein interaction screens; and evaluation of siRNA libraries. While RNA-Seq whole transcriptome analysis has yet to be reported for host cells infected with RABV, several other array-based and proteome studies have been performed with RABV. Of the four transcriptome studies performed, they all have identified increased expression of genes involved in immune regulation [13–16]. Profiling protein expression identifies factors involved in ion homeostasis and synaptic physiology [17]; cytoskeletal, antioxidative stress, regulatory, and protein synthesis genes [18]; and cell regulation and calcium homeostasis [19]. Unfortunately, while both transcriptome and proteome approaches were developed to identify differentially expressed genes and proteins, once these have been identified, their "functional relevance to rabies pathogenesis is unclear [16]." Most of the products identified in these studies have little direct effect on viral infection/replication. Hence, they lack specificity as they do not necessarily identify host-based targets with a measurable phenotypic effect on infection. Approaches to identify host-based viral protein binding partners including Y2H and a newer technique that uses a cell-free protein synthesis (CFPS) method have also been used with RABV. Unfortunately, they yield very few targets as by their very nature, they only identify those host-based targets that directly interact with viral proteins, meaning that most host-based factors involved in infection are not evaluated. For example, Y2H using RABV P as bait has identified three RV targets (STAT1, IRF3, and FAK) [20]. Y2H systems are further limited in that they require a transcriptional reporter to localize to the nucleus, complicating analysis of membrane proteins; and lack post-translational modifications which contributes to the decreased detection rate of about a fourth of all estimated interactions (reviewed by [21]). The very recently developed CFPS method has only identified one target: ABCE1 [22].

Screening mutant libraries of stem cells has advantages over these technologies as stem cells have stable mutations and knockdown of targets and provide all necessary intracellular localizations and mammalian post-translational modifications. In addition, stem-cell-derived neurons represent relevant model systems as they form functional networks of synaptically coupled cells that have electrophysiological and biochemical properties almost indistinguishable from primary cultures of embryonic central nervous system neurons [23]. While differentiated neurons have already been screened to discover new drug compounds [24]; the creation and screening of a large panel of differentiated mutant neurons has not been described.

Thus, in order to evaluate the potential for screening mutant libraries for host-based targets, we develop a green fluorescent protein (GFP)-based rabies infection assay and demonstrate that the heterozygous nature of the gene trap mutation is not a limitation as it provides a robust, reproducible phenotype. In addition, we are able to shift the culturing and differentiation processes into multiwell plates such that they can be performed simultaneously for hundreds or thousands of clones, making the task routine. To evaluate the robustness of the phenotype, we chose control clones with mutations known to play a role in infection and differentiated them into neurons and assayed them for sensitivity to rabies infection. A Mavs (Mitochondrial antiviral signaling protein) mutant showed increased viral activity in our assay; silencing of Mavs expression is known to permit viral replication [25]. In contrast, Ncam and Ngfr (RABV receptors) indicate decreased viral activity as does a *Dynll2* (*dynein light chain LC8-type 2*) mutant clone. Hence, the heterozygous mutations in our library yield robust and expected phenotypes. Next, we defined a subset of more than 3,200 gene-trap clones, optimized methods to culture and differentiate them into neurons simultaneously, and assayed them by high-content analysis for sensitivity to GFP-labeled RABV over time. After all the cell lines were screened, 63 host targets were identified. We used siRNA knockdown of *Unc13d* and *Bbs4* in wild-type ESCs and primary cultures of embryonic spinal cord neurons to validate that reduction of gene-expression is indeed the mechanism through which hits result in altered sensitivity to RABV. Hence, this technique was effective in discovering host-based genes involved in the infection process and these protocols have wide applicability for a variety of agents (viral, bacterial, toxin, or drug) and endpoint assays.

Materials and Methods

ESC Expansion

Library clones were pulled from liquid nitrogen freezers and grown on 24-well plates coated with mouse embryonic fibroblasts (MEFs) in media containing leukemia inhibitory factor (LIF) to prevent differentiation. Media consisted of Dulbecco's modified eagle media (DMEM) supplemented with L-glutamine (200 nM in 85% NaCl solution), 100× nucleotides, nonessential amino acids (100×), penicillin/streptomycin (10,000 U Pen/ml, 10,000 μg Strep), sodium pyruvate (100 mM), and LIF (10 μg in 1 ml sterile H_2O). Media were changed daily, and the plates were passaged every other day. When cells were 85% confluent, they were trypsinized and frozen in quadruplicate in barcoded 0.5 ml screw-cap tubes in Freeze media overlaid with mineral oil. Upon rethaw, cells were passaged two to three times on MEFs and once on gel prior to plating at approximately 10,000 cells per well into two adjacent wells of 96-well optical plates coated with gelatin for assays.

Differentiation into Embryonic Stem-Cell-Derived Neurons

Cells were thawed and passaged two to three times on MEFs and two to three times on gel to remove feeders. Cells were then trypsinized, counted, and suspended in mouse embryonic stem cell serum replacement media (MES/SR) media (DMEM/F-12 supplemented with 15% knockout serum replacement, nonessential amino acids [100×], sodium pyruvate [100 mM], 2-ME [1,000×], and penicillin/streptomycin [1/2×]) on ultra-low attachment 24-well plates at a confluence of 250,000 cells per 1.5 ml media. The plates were incubated at 37°C and left on a rotary shaker to allow for the formation of cellular aggregates. On days 2 and 5, plates were tilted at an approximate 45°C angle for 5 minutes to allow aggregates to settle by gravity and media were exchanged with fresh MES/SR containing 1 μl retinoic acid per ml (5 μM final concentration) to encourage neuronal differentiation. Then, on day 6, media were aspirated and aggregates dissolved with 0.5 ml Accutase and resuspended in Neurobasal-A media supplemented with B27 (50×), cAMP (1 mM), GDNF (10 μg/ml), and penicillin/streptomycin (1/2× or 5,000 U Pen/ml, 5,000 μg Strep). Aggregates were broken up by trituration with a 5 ml serologic pipet. We found that the large bore was necessary for further culture. Cells were strained, counted, and plated at a confluence of 100,000 cells/well on 96-well plates previously coated with a 1:10 Matrigel dilution in NS media. The media were changed after 16–24 hours. Cultures were allowed to differentiate for 9 days prior to infection and fed every 3–4 days.

Neuron Characterization and Immunocytochemistry

Following differentiation, neurons were stained with cell-type and protein-specific antibodies. Briefly, cells were rinsed with phosphate buffered saline (PBS), fixed in 4% paraformaldehyde for 20 minutes at RT, rinsed with PBS, permeabilized for 5–10 minutes in 0.1% Triton X-100 in PBS, rinsed in PBS, blocked with goat serum for 30 minutes at RT, incubated with primary antibody overnight at 4°C. The following day, excess primary antibody was rinsed off with PBS and fluorescent secondary antibody was incubated at 1:1,000 dilution for 30 minutes at RT in the dark. Cells were rinsed in PBS, stained with Hoechst at 1:20,000 for 5 minutes and rinsed with PBS prior to imaging. Cells were stored indefinitely at 4°C in PBS. The following primary antibodies were used at respective dilutions: vGlut-2 from Synaptic Systems (Goettingen, Germany; www.sysy.com) at 1:500, TH from Millipore (Darmstadt, Germany; www.emdmillipore.com) at 1:100, glial fibrillary acidic protein from Millipore at 1:100, PSD95 from Millipore at 1:100, Synaptophysin from Millipore at 1:500, SERT from Millipore at 1:500, ChAT from Millipore at 1:200, GAD65/67 from Millipore at 1:500, GATA at 1:100, GABA(A) from Millipore at 1:500, NGFR p75 from Millipore at 1:250, Ncam from Millipore at 1:250, Chrna7 from Abcam (Cambridge, MA; www.abcam.com) at 1:250, Tuj-1 from BD Pharmingen (Piscataway, NJ; www.bdbiosciences.com) at 1:500, Map2 from Synaptic Systems at 1:200, and anti-rabies Glycoprotein from Millipore at 1:250. Fluorescent secondary antibodies include: anti-rabbit, anti-mouse, and anti-goat diluted 1:1,000.

Clone Selection

Because most genes that are represented in the gene-trap library have more than one clone, we designed a bioinformatics method to select a representative subset of clones for screening. All the clones were ranked based on relevant characteristics to identify the top clone for each gene in the library. Clones were first selected that mapped to consistent genomic coordinates based on sequencing of PCR products adjacent to both ends of the insertion vector. Then a Blast search was used to determine which matches were statistically significant (*E*-value $<$ 1e-20), and to rule out clones that mapped ambiguously to repetitive regions. As many genes have alternative transcripts due to alternative start sites and alternative splicing, we selected traps that are predicted to disrupt at least 60% of possible transcript (variant) forms from a gene. Finally, we required traps to occur within the first half of the coding region (exons) of the gene of interest. The clones meeting these criteria were then ranked based on proximity of the insertion site to the start codon.

A total of 3,200 clones were selected for screening. Approximately one-third of the clones were prioritized based on relevant functional classifications, and the other clones were chosen on a random basis for coverage of the genome. Gene ontology terms associated with gene annotations were used to select 1,150 genes with functions plausibly relevant to rabies infection or activity, including: GTPase activity (GO:0003924), regulation of neurotransmitter levels (GO:0001505), endocytosis/exocytosis (GO:0006897), cytoskeletal structure (GO:0044430), receptor or kinase activity (GO:0004872, GO:0016301), vesicle-mediated transport (GO:0016192), endosome to golgi retrograde transport (GO:0042147), neuron homeostasis (GO:0070050), neuron apoptosis (GO:0051402), neurotransmitter uptake (GO:0001504), cell surface receptor linked signaling pathway (GO:0007166), vesicle activity (GO:0031982), immune response (GO:0006955), and response to virus (GO:0009615). An additional 2,050 clones were selected at random among the remaining genes in the mouse genome to create an unbiased sample, with the constraint that at most one clone (the one closest to the start codon) was selected per gene.

Rabies Infection/Replication Time Course Assay

Both undifferentiated cells and neurons were infected and assayed. We used the attenuated SPBN-Nfu-GFP labeled RABV

(a kind gift of Dr. Mattias Schnell) which was labeled with green fluorescent protein for imaging purposes. Undifferentiated cells were plated at 10,000 cells cell per well on a 96-well optical plate coated with gelatin and neural precursor cells were plated at 100,000 cells per well on a 96-well optical plate coated with 1:10 Matrigel. Undifferentiated cells were infected 16–24 hours after plating and neurons were infected 9 days after plating to allow for differentiation. We infected cells with 1 multiplicity of infection (MOI) of virus, let them incubate for an hour, then aspirated the virus, and added fresh virus-free media. The cells were then returned to the incubator and imaged at 24, 48, and 72 hours, with one-quarter volume fresh media added at the 48-hour mark. After 72 hours, the media were collected and used in the viral shedding assay. All cells were fixed and nuclei stained with Hoechst (1:20,000) for imaging. Neurons were also stained with fluorescent Tuj-1.

Rabies Viral Shedding Assay

Media from the time course assay were collected after 72 hours and transferred to new wild-type ESCs to evaluate shedding. Fresh ESCs were plated at 10,000 cells per well on 96-well optical plates coated with gelatin 3–6 hours prior to infection. Media were allowed to infect the cells for 48 hours, after which cells were fixed with 4% paraformaldehyde, stained with Hoechst 1:20,000 and imaged.

Screening Strategy and Data Analysis for Undifferentiated ESCs

After the initial round of screening for the 2,680 ESC clones, mean *Z* and *B*-scores were calculated on a per plate basis to normalize for plate-to-plate variability and to adjust for plate-specific biases [26]. *Z*-scores were calculated using the following equation: $Z = (\chi - \mu)/\sigma$ where $\chi =$ the intensity of the clone of interest, $\mu =$ the mean intensity of the population, and $\sigma =$ the SD of the intensity of the population. For first pass analysis, a normalized value for each plate imaged was created. Clone's individual *Z*-scores were the result of their value divided by this normalized value. We also used a *B*-score to normalize data. It is calculated as the residual (defined as the difference between the observed value and the fitted value) divided by the median absolute deviation [26]. It is a robust analog of the *Z*-score that is more resistant to the presence of outliers and more robust to differences in the measurement error distributions of the clones. Cut-off values for the definition of hits for the first round of screening were as follows: 24-hour time point: $Z < -1.5$ or $Z > 3$ and $B < -1.5$ or $B > 6$; 48 hours time point: $Z < -1.75$ or $Z > 2.5$ and $B < -2$ or $B > 6$; 72-hour time point: $Z < -2$ or $Z > 2.3$ and $B < -2.4$ or $B > 4.91$. These criteria resulted in 114 unique clones being selected. Shedding hits were defined by criteria of $Z < -1.3$ or $Z > 3$. This involved 43 unique clones. All assays were repeated during a second round of screening for these hits. Again, mean *Z* scores were calculated; however, secondary screening analysis differed from primary analysis in that the normalized *Z*-score values for each plate were obtained from infected wild-type cells; individual clone values were then compared to this normalized wild-type *Z* score to generate a final *Z* score used to determine levels of sensitivity and/or resistance. Cut-off values for mean *Z* score were as follows: 24-hour time point: $Z < -1.5$ or $Z > 2.8$; 48-hour time point: $Z < -1.73$ or $Z > 1.54$; 72-hour time point: $Z < -1.29$ or $Z > 1.54$. Secondary screen shedding hits were defined by criteria of $Z < -1.5$ or $Z > 1.97$.

Screening Strategy and Data Analysis for Neurons

After the initial round of screening for the 1,870 differentiated neurons, mean *Z* and *B*-scores were calculated on a per plate basis. Cut-off values for the definition of hits for the first round of screening were as follows: 24-hour time point: $Z < -1.5$ or $Z > 3$; 48-hour time point: $Z < -1.75$ or $Z > 3$; 72-hour time point: $Z < -1.75$ or $Z > 3$. Shedding hits were defined by criteria of $Z < -1.4$ or $Z > 3.0$. All assays were repeated during a second round of screening for these hits. Again, mean *Z* scores were calculated; however, secondary screening analysis differed from primary analysis in that the normalized values for each plate were obtained from infected wild-type cells; individual clone values were then compared to this normalized wild-type *Z* score to generate a final *Z* score used to determine levels of sensitivity and/or resistance. Cut-off values for the second round of screening were as follows: 24-hour time point: $Z < -2.5$ or $Z > 1.5$; 48-hour time point: $Z < -3.0$ or $Z > 1.5$; 72-hour time point: $Z < -3$ or $Z > 2.2$. Shedding hits were similarly defined and $Z > 3.8$.

High-Content Imaging and Analysis

Rabies infection/replication time course assays and shedding assays were evaluated by intracellular fluorescence of the GFP-labeled virus using a GE 2000 High-Content Analysis System. We used FITC, DAPI (4′,6-diamidino-2-phenylindole), Texas Red, and Brightfield settings. Brightfield was used view cells, FITC to identify the GFP-virus, DAPI for nuclei, and Texas red for the Tuj-1 (Fluro555-conjugated Tuj-1 from BD Pharmingen) stained neurons. Images were captured for 12 randomized fields of view per well for all plates and assays using the 20× high NA objective. For undifferentiated cells and neurons, we quantitated FITC intensity as a function of density multiplied by area.

Gene Ontology Analysis

Gene ontology (GO), the de facto standard in gene functionality description, is used widely in functional annotation and enrichment analysis. We used the GO terms associated with hits to look at functional enrichment. For each positive clone and its GO term, we assessed the counts and percentages of genes matching each GO term within the main pool of genes and the subset of hits for each screen. "Height" gives a sense of how high (close to the root) a particular GO Term is; with smaller values indicating closeness to the root. The closer to the root/beginning of the hierarchy, the more general the GO terms (e.g., molecular—function, or biological process); thus, Height < 3 were excluded. We calculated a *Z*-score based on expected versus observed counts, and a *p*-value. Sorting based on *Z*-score shows the GO terms with the biggest differences; however, this *Z*-score could be very high for GO terms with small relative number of matches. Hence, those with only one match were excluded. Next, we sorted based on percentage of the Hits with highest percentage on top and defined groups of genes where we see enrichment.

Secondary Assays for RABV

Dose response assays were also performed on hits. We used MOIs of 0.1, 0.5, 1, 5, and 10 for infection of both

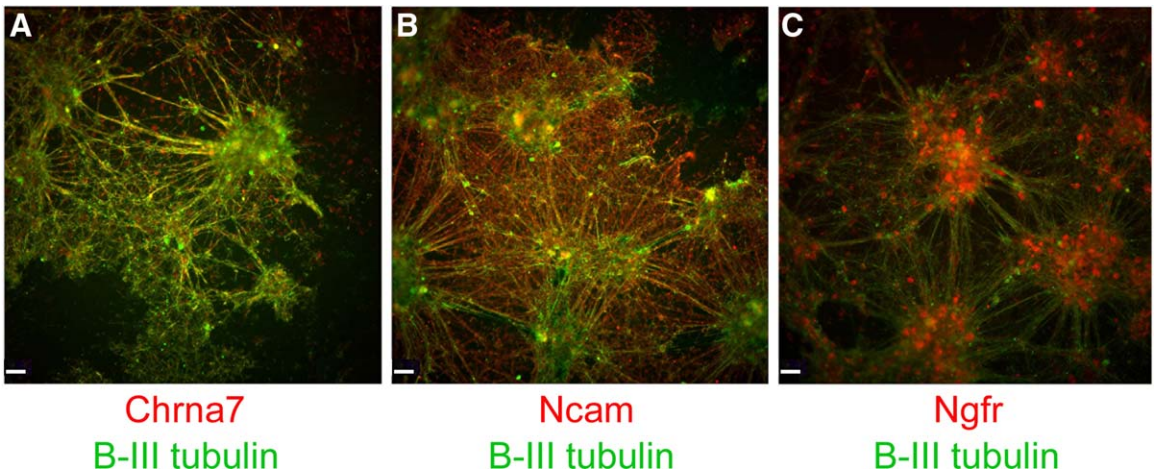

Figure 1. Characterization of differentiated neurons. **(A–C):** Immunocytochemistry on wild-type embryonic stem cells that were differentiated into neurons showing expression of B-III tubulin (A–C) (FITC-green) and known rabies virus receptors Chrna7 (A), Ncam (B), and Ngfr (C) (Texas Red). Yellow signals indicate colocalization of green and red markers. The scale bar represents 30 μm.

undifferentiated cells and neurons and imaged plates at 24, 48, and 72 hours. We also performed cell replication studies. ESCs for each clone were thawed and passed two times on MEFs and two times on gel prior to plating on gel at 30,000 cells per 24-well. Cells were trypsinized and counted at 24, 48, and 72 hours to compare growth rates.

siRNA Validation

Predesigned siRNA duplexes to specific targets were obtained from Integrated DNA Technologies (San Jose, CA; www.idtdna.com) and 30 nM of each duplex was transfected into cells (wild-type ESC or primary embryonic spinal cord neurons) with Lipofectamine RNAiMAX (Invitrogen) (Grand Island, NY; www.lifetechnologies.com) according the manufacturer's directions at least 48 hours prior to RABV infection. RABV assays for infection, replication, and shedding were performed as described above. RNA was extracted from some wells using a Qiagen RNEasy Kit and knockdown of gene expression was evaluated using predesigned gene-specific Qiagen (Venlo, Limburg; www.qiagen.com) QuantitTect primer assays and Q-RT-PCR. Transcript quantities were determined using the ddCt method and compared to Hprt as the housekeeping gene.

Results

Selection of Clones, Expansion, and Differentiation into ESC-Derived Neurons

A subset of 3,200 mutant ESCs was assembled [2]. We applied a multitiered computational filter that selected one clone with high quality sequence tags per gene. Gene-traps were required to disrupt at least 60% of the transcripts predicted for the gene and to occur within the first half of the coding region (exons) of the gene of interest. Approximately one-third (1,150 genes) of the set were prioritized based on relevant functional classifications using GO terms, such as response to virus, receptor, or immune response (see Materials and Methods for all specific GO terms). An additional 2,050 clones were selected at random from the remaining genes to create an unbiased sample.

Initial clone recovery was asynchronous; however, it was clear that recovery, expansion, and synchronization were critical to simultaneous differentiation and subsequent assay performance. Hence, we worked with sets of 196 clones and staggered thaw dates to allow for weekly processing. When cells were expanded and 85% confluent, they were frozen in quadruplicate. Clones (2,680) were viable and readily expanded. Upon rethaw, these clones were more efficiently recovered and synchronized by two to three passages on MEFs to prevent differentiation, followed by one passage on gel for subsequent use in assays. We used published differentiation protocols that have successfully generated neurons from murine ESCs [27, 28]. We modified protocols by reducing culture sizes to optimize throughput. Cells were plated in suspension with retinoic acid and without serum on a rotary shaker to form cellular aggregates. After 6 days, aggregates were dissolved and neuronal precursors were plated and allowed to differentiate for 9 days prior to assays. Figure 1A–1C shows cells that are positive for the neuron-specific maker B-III tubulin and rabies receptors (NGFR p75, Ncam, and Chrna7) which are highly expressed in neurons. Furthermore, cells demonstrate structural morphology typical of neurons. Supporting Information Figure S1 shows that resultant cultures are pan-neuronal and positive for the following neuron-specific immunohistochemical markers: Tuj-1, Map2, vGlut-2, PSD95, Synaptophysin, SERT, ChAT, and GAD65/67. These markers are typically used as controls to verify neuron identity. A total of 1,870 clones were readily differentiated and screened.

Assay Development and Screening Strategy

First, a high-content, high-throughput assay for RABV was developed. Using viruses expressing GFP and other visual markers such as luciferase for various detection and high-content assays to measure viral infection and/or replication is a well-established method. More specifically, GFP-rabies and the resultant GFP levels have been used to measure titers of virus-neutralizing antibodies in serum samples [29]. Khawplod et al. explicitly showed that GFP levels directly correlate to virus levels as titers based on GFP quantitation have a direct linear correlation to titers determined by the gold-standard rapid fluorescent focus inhibition test approved by WHO. We used the attenuated SPBN-Nfu-GFP labeled RABV (a kind gift of Dr. Mattias Schnell) [30]. To develop our high-content live

imaging assay, we first showed that there is a direct correlation between GFP expression intensity and anti-Rabies glycoprotein expression intensity. PC-12 neuronal cells were infected with various MOIs of GFP-virus and fixed and stained with anti-rabies Glycoprotein 48 hours later. Image analysis using a GE INCell 2000 high-content imager to quantitate both GFP intensity and anti-glycoprotein intensity indicated a direct correlation (Fig. 2A). Next, we showed that GFP intensity follows time and dose course trends by infecting ESCs with various MOIs of virus and performing live imaging over time (Fig. 2B). Live GFP intensity levels were assessed at 24 hours to get a sense of initial infection and again at 48 and 72 hours to assess time points corresponding to intracellular replication. We tracked the same fields of cells over time. Additionally, as a measure of the viral shedding process, supernatants from 72-hour cultures were transferred to fresh wild-type ESCs which were evaluated for GFP-expression after an additional 48 hours. Even though this final shedding assay analysis occurs 5 days after the initial infection, we see quantitative dose response correlation based on the initial MOI. Furthermore, the dose response assays allowed us to determine that an MOI of 1 is appropriate for our assay. MOIs of 5 and 10 showed potential to saturate the cultures by 72 hours and an MOI of 0.5 was not easily detectable at 24 hours. Evaluation of live time course images indicates that changes in GFP intensity over time are a result of GFP-virus spreading to new cells (Fig. 2C). Approximately three cells are expressing high levels of GFP at 24 hours, by 48 hours a cluster of several dozen cells is expressing GFP at high levels and by 72 hours, hundreds of cells are expressing GFP. Live time-lapse imaging was used throughout the screen and we were able to visualize the same fields of view over the 24, 48, and 72 hours time course.

Four mutant clones with known roles in rabies or viral infection were selected as controls to validate the assay: Mavs (mitochondrial antiviral signaling protein), Ncam (neural cell adhesion molecule), Ngfr (nerve growth factor receptor), and Dynll2 (dynein light chain LC8-type 2) (Fig. 2D). Silencing of Mavs expression is known to permit viral replication [25]. Indeed, after RABV infection, the Mavs mutant clone showed increased viral activity and a *Z*-score of GFP-fluorescence of 8.78 in comparison to wild-type clones indicating sensitivity to intracellular replication at 72 hours. Ncam and Ngfr are known RABV receptors [9]. Subsequent to infection, Ncam and Ngfr mutant clone *Z*-scores are as low as $Z = -5.68$ and -5.89, respectively. Decreased GFP intensity can be interpreted as a partial decrease in viral activity, although not absolute resistance. Finally, the RABV phosphoprotein contains a dynein light chain 8 binding motif that promotes efficient viral transcription [11]. When Dynll2 mutant clones are infected, they are relatively resistant with $Z = -6.09$. Hence, results with these known clones that yield the anticipated relatively sensitive and resistant phenotypes indicate that the assay works and, most importantly, that the heterozygous mutations in our library yield robust phenotypes.

In order to evaluate cell-type specificity of the interactome, cells were screened in two states of differentiation: pluripotent undifferentiated ESCs and neurons. Screening began with more than 2,680 pluripotent ESC lines and 1,870 differentiated neuron cultures. After the initial screen, *Z*-scores were calculated to identify the most divergent 5% of clones demonstrating maximum and minimum resistance (150 ES and 120 neuron clones; see Materials and Methods for detailed cut-off values). Figure 3 and Supporting Information Figure S2 depict neuron and undifferentiated ESC clones, respectively, showing sensitivity and resistance to GFP-RABV infection at 24, 48, 72 hours, and in the shedding assay. All hits were retested in a second round of screening that repeated all assay time points in both cell types. Table 1 lists gene-traps which repeatedly showed phenotypes after two rounds of assays. Genes are listed by time point and segregated based on relatively sensitive or resistant phenotypes. For example, the mutant Cib1 (calcium and integrin binding protein 1) clone confers resistance at both 48 and 72 hours. CIB1 is implicated in Kaposi's Sarcoma-associated herpes virus entry and macropinocytosis [31]. Conversely, the Pick1 (protein interacting with C kinase 1) clone is sensitive to infection; and Pick1 binds coxsackie B virus and adenovirus receptors [32].

Secondary assays were performed to further characterize clones and the platform. Viral dose response data indicated that the degree of infection correlates with the initial MOI; Figure 4A–4D. As these assays were performed on both sensitive and resistant clones, there was considerable clone-to-clone variability; although resistant clones have lower levels of infection than sensitive clones, especially at the originally tested MOI of 1. This data support the reproducibility of the high content analysis assay. We also noticed saturation of response in neurons by 72 hours, as increasing MOI no longer increased infection (Fig. 3D). Cell replication studies in undifferentiated cells showed variability in doubling rates, but there was no trend in correlation between doubling rate and *Z*-scores for rabies sensitivity, thus eliminating this as a primary confounding variable (Fig. 4E).

Platform Validation

siRNA duplexes were used as a confirmatory assay. A subset of 10 genes was selected to represent a cross-section of the hits such that there was broad coverage between clones showing relatively high levels of sensitivity and resistance in each of the cell types and each of the multiple assays (Supporting Information Table S1). To expedite validation, cells were treated with the various siRNAs, rescreened for sensitivity for RABV, and knockdown of target was verified by Q-RT-PCR. The first clones to both repeat the phenotype after one round of siRNA transfection and demonstrate loss of gene product were immediately prioritized; other clones have been set aside for further development at a later time. *Unc13d* and *Bbs4* siRNA were found to induce resistance to RABV infection in both wild-type ESCs and primary spinal cord neurons. *Unc13d* was originally identified as a clone of interest at both the 24 and 72 hours time points in ESCs. When *Unc13d* siRNA was added to wild-type ESCs, it resulted in 41%, 70%, and 65% less fluorescence at 24 hours, 48 hours, 72 hours, respectively, and 45% less in the shedding assay. Up to 80% knockdown was observed based on qRT-PCR. The assay was repeated a second time and similar results were obtained. When primary spinal cord neurons were transfected, up to 60% knockdown of the transcript was achieved, and 92%, 30%, and 45% reduction in fluorescence was observed at 24 hours, 48 hours, 72 hours, respectively, and 69% less in shedding. *Bbs4* (Bardet-Biedl syndrome 4) was originally identified

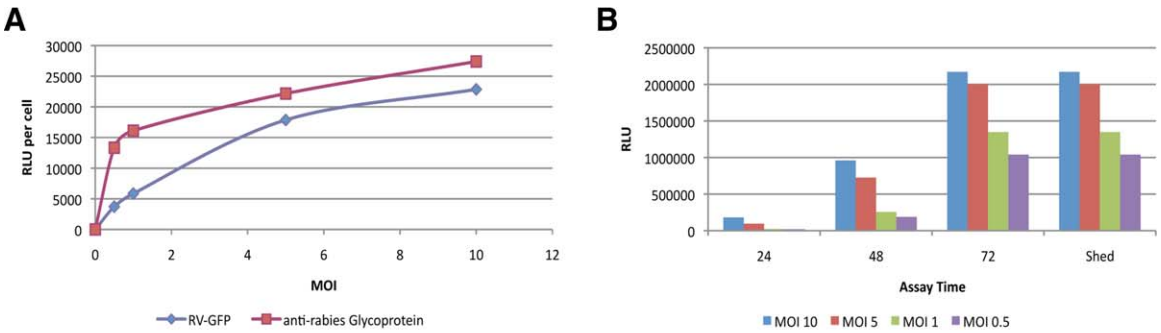

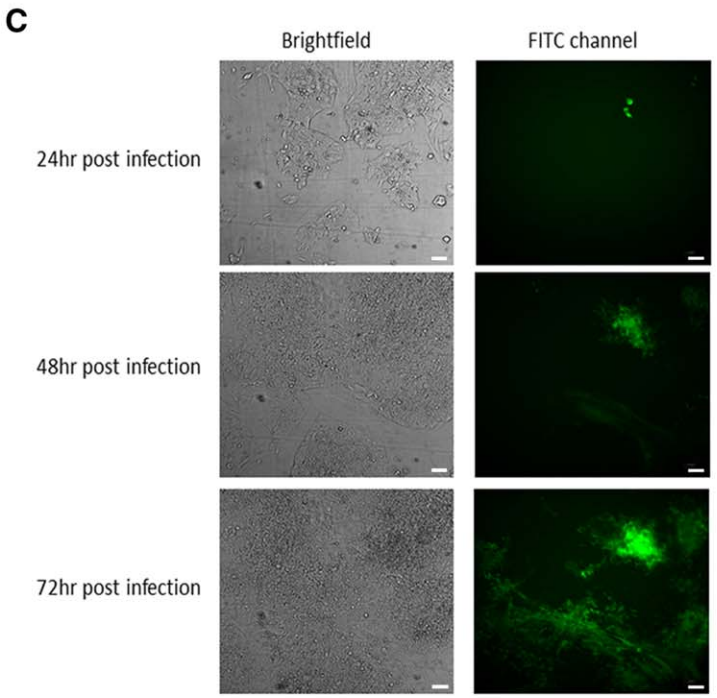

D

	24 hour	48 hour	72 hour	Shed
Mavs	7.06	6.88	8.78	-1.95
Dynll2	-2.33	-6.09	-5.79	-0.94
Ncam	-2.99	-4.4	-5.68	0.15
Ngfr	-3.96	-4.62	-5.89	-2.9

Figure 2. Development of GFP-RV high content analysis assay. **(A)**: Direct correlation between GFP-RV-intensity and anti-rabies Glycoprotein expression. PC-12 cells were infected with various indicated MOIs of GFP labeled rabies virus. Cells were fixed after 48 hours and stained with primary anti-rabies glycoprotein. Image analysis for both GFP intensity and anti-Glycoprotein intensity indicates a direct correlation between anti-rabies glycoprotein and GFP expression. **(B):** RV-GFP intensity follows time and dose response trends in embryonic stem cells (ESCs). Cells were infected with various MOIs (0.5, 1, 5, and 10). Live GFP levels were assessed at 24 hours to get a sense of initial infection and again at 48 and 72 hours to assess time points corresponding to intracellular replication using a GE INCell 2000 high-content imager, to track the same cells over time. Additionally, as a measure of the viral shedding process, supernatants from 72-hour cultures were transferred to fresh wild-type ESCs which were evaluated for GFP-expression after an additional 48 hours. **(C):** Time lapse imaging data support that increasing GFP intensity is due to virus spread. Live time-lapse imaging was used throughout the screen and we were able to visualize the same fields of view over the 24, 48, and 72 hour time course. The number of GFP-positive cells increases over time. The scale bar represents 30 μm. **(D):** Performance (*Z*-scores; compared to wild type) of control clones mutant for genes known to be involved in rabies virus infection in assays. Abbreviations: GFP, green fluorescent protein; MOI, multiplicity of infection.

as a clone of interest at both 24 and 48 hours in neurons. When siRNA was added to primary spinal cord neurons up to 58% knockdown was obtained based on qRT-PCR and 37%, 57%, and 74% less fluorescence was observed at 24 hours, 48 hours, and 72 hours, respectively. The assay was repeated and similar results were obtained. These assays confirm that

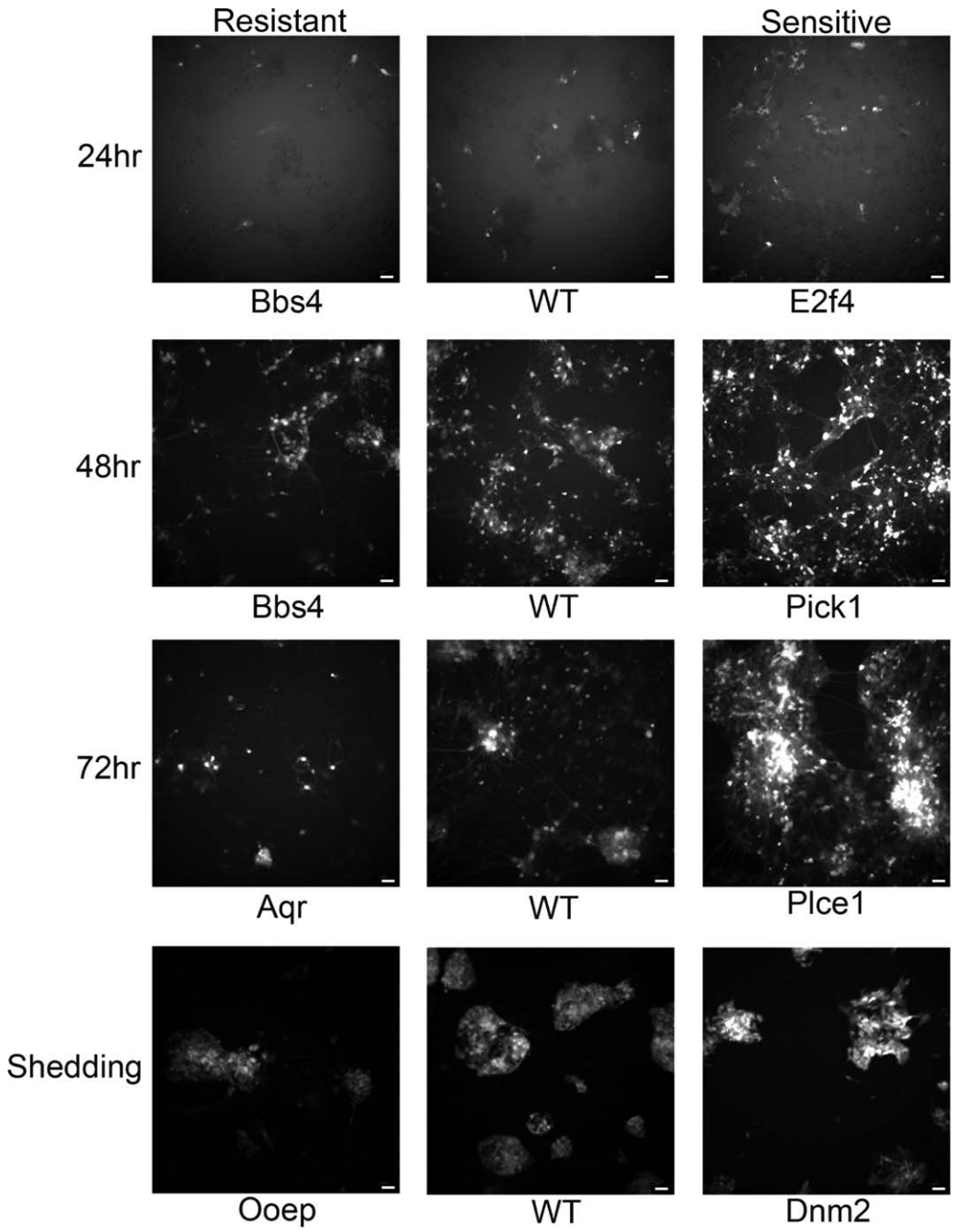

Figure 3. Example images of neurons defined as hits showing sensitivity and resistance to green fluorescent protein (GFP)-Rabies virus infection at 24, 48, 72 hours, and in a shedding assay. Examples of WT clones are shown in the middle column for comparison. Resistant clones are in the left column and sensitive clones are in the right column. Clone names are indicated beneath each image. Images show relative GFP intensity and are indicative of the amount of infection. Cells shown in shedding assays are WT ESCs infected with virus shed into supernatant from clone-specific neuron cultures. The scale bar represents 30 μm. Abbreviation: WT, wild type.

decreased expression of host targets is indeed involved in sensitivity to RABV infection.

Discussion

Of the 63 host-based genes identified, all are novel RABV targets, as they have not been associated with RABV infection. At least 19 of these have little or no known function, that is, cDNAs or predicted genes. Nine targets that modulate host cell response to rabies have documented roles in viral infection. These genes and their roles are detailed in Table 2 and include: *Pick1* [32], *Aqr* [33], Rab5 [34], Cib1 [31], *Dapk1* [35, 36], *Cux1* [37, 38], *Fbxw7*[39], *Rb1*[39], and *E2f4* [39–41]. Of the remaining 44 genes, targets include cell surface receptors (*Tm231*); genes involved in innate immunity (*Cort* and *Unc13d*); transcription factors (*Cux1*, *E2f4*, *Rcor2*, and *Olig2*); intracellular trafficking genes (*Rab5b*); members of critical

Table 1. Hits which repeatedly showed phenotypes after two rounds of screening assays

Resistant				Sensitive			
Symbol	**Gene**	***Z*-score**	**Cell**	**Symbol**	**Gene**	***Z*-score**	**Cell**
24 hours							
Cux1	Cut-like homeobox 1	−2.00	ES	Tmem231	Transmembrane protein 231	3.69	ES
Unc13d	Unc-13 homolog D (*Caenorhabditis elegans*)	−1.55	ES	2310004I24Rik	RIKEN cDNA	3.75	ES
Iws1	Iws1 homolog (*Saccharomyces cerevisiae*)	−2.35	ES	Morc1	Microrchidia 1	4.53	Neuron
Gm11630	Predicted gene 11630	−2.32	Neuron	Fbxw7	F-Box and WD40 Domain Protein 7	9.64	Neuron
1810013L24Rik	RIKEN cDNA	−3.19	Neuron	4930432O21Rik	RIKEN cDNA	6.75	Neuron
Cisd2	CDGSH iron sulfur domain 2	−2.50	Neuron	E2f4	E2F transcription factor 4	9.38	Neuron
Bbs4	Bardet-Biedl syndrome 4	−2.19	Neuron				
1810022K09Rik	RIKEN cDNA	−3.84	Neuron				
48 hours							
Dtx3	Deltex 3 homolog (Drosophila)	−1.93	ES	Pfdn2	Prefoldin 2	2.84	ES
Rnf121	Ring finger protein 121	−1.83	ES	Aaas	Achalasia, adrenocortical insufficiency, alacrimia	2.66	ES
Gnai3	Guanine nucleotide binding protein (G protein), alpha inhibiting 3	−6.09	Neuron	Gm12258	Predicted gene 12258	2.84	ES
Cib1	Calcium and integrin binding 1 (calmyrin)	−2.33	Neuron	Lyrm7	LYR motif containing 7	4.73	ES
Fn3krp	Fructosamine 3 kinase-related protein	−1.81	Neuron	Rcor2	REST corepressor 2	5.24	ES
1700055D18Rik	RIKEN cDNA	−3.74	Neuron	Fam173b	Family with sequence similarity 173, member B	4.26	ES
Ccdc124	Coiled-coil domain containing 124	−5.81	Neuron	Usp1	Ubiquitin-specific peptidase 1	3.82	Neuron
Mrps15	Mitochondrial ribosomal protein S15	−3.62	Neuron	Ufc1	Ubiquitin-fold modifier-conjugating enzyme 1	4.03	Neuron
Gm9631	Predicted gene 9631	−4.58	Neuron	Rb1	Retinoblastoma 1	3.97	Neuron
2310003C23Rik	RIKEN cDNA	−3.59	Neuron	Rab5b	Ras-associated protein Rab5b	3.94	Neuron
Gm11630	Predicted gene 11630	−6.30	Neuron	Pick1	Protein interacting with C kinase 1	6.80	Neuron
1810013L24Rik	RIKEN cDNA	−6.58	Neuron	Plce1	Phospholipase C, epsilon 1	8.97	Neuron
Aqr	Aquarius	−6.26	Neuron	9430023L20Rik	RIKEN cDNA	4.01	Neuron
9130208E07Rik	RIKEN cDNA	−7.40	Neuron				
Bbs4	Bardet-Biedl syndrome 4	−4.09	Neuron				
Cisd2	CDGSH iron sulfur domain 2	−2.62	Neuron				
Rpa2	Replication protein A2	−3.43	Neuron				
Smtn	Smoothelin	−3.39	Neuron				
1810022K09Rik	RIKEN cDNA	−6.88	Neuron				
72 hours							
Rad51l3	RAD51 homolog D	−2.10	ES	1700017B05Rik	RIKEN cDNA	2.48	ES
Dtx3	Deltex 3 homolog (Drosophila)	−2.03	ES	2610001J05Rik	RIKEN cDNA	2.29	ES
Dapk1	Death-associated protein kinase 1	−2.14	ES	Rcor2	REST corepressor 2	2.84	ES
Unc13d	Unc-13 homolog D (*C. elegans*)	−2.81	ES	Sap30bp	SAP30 binding protein	3.73	ES
Gnai3	Guanine nucleotide binding protein (G protein), alpha inhibiting 3	−6.04	Neuron	Usp1	Ubiquitin-specific peptidase 1	6.59	Neuron
Brcc3	BRCA1/BRCA2-containing complex, subunit 3	−4.67	Neuron	Ufc1	Ubiquitin-fold modifier-conjugating enzyme 1	4.30	Neuron
Cib1	Calcium and integrin binding 1 (calmyrin)	−2.30	Neuron	Rab5b	Ras-associated protein Rab5b	4.69	Neuron
Fn3krp	Fructosamine 3 kinase-related protein	−2.04	Neuron	Pick1	Protein interacting with C kinase 1	5.23	Neuron
1700055D18Rik	RIKEN cDNA	−3.70	Neuron	Plce1	Phospholipase C, epsilon 1	11.11	Neuron
Ccdc124	Coiled-coil domain containing 124	−5.74	Neuron				
Mrps15		−3.62	Neuron				

Table 1. *Continued*

Resistant				Sensitive			
Symbol	**Gene**	***Z*-score**	**Cell**	**Symbol**	**Gene**	***Z*-score**	**Cell**
	Mitochondrial ribosomal protein S15						
Sept1	Septin 1	−1.78	Neuron				
4833418A01Rik	RIKEN cDNA	−2.07	Neuron				
Gm9631	Predicted gene 9631	−5.04	Neuron				
Tmprss12	Transmembrane (C-terminal) protease, serine 12	−6.54	Neuron				
2310003C23Rik	RIKEN cDNA	−3.62	Neuron				
Gm11630	Predicted gene 11630	−6.40	Neuron				
Aqr	Aquarius	−5.14	Neuron				
9130208E07Rik	RIKEN cDNA	−7.02	Neuron				
Cisd2	CDGSH iron sulfur domain 2	−2.34	Neuron				
Rpa2	Replication protein A2	−4.47	Neuron				
1810022K09Rik	RIKEN cDNA	−8.68	Neuron				
Shed							
Tpm3	Tropomyosin 3, gamma	−2.10	ES	Mrpl28	Mitochondrial ribosomal protein L28	5.04	ES
Usp33	Ubiquitin-specific peptidase 33	−1.87	ES	Galntl1	UDP-*N*-acetyl-alpha-D-galactosamine:polypeptide *N*-acetylgalactosaminyltransferase 1	5.17	ES
C77080	Expressed sequence C77080	−1.77	ES	Sesn1	Sestrin 1	5.19	ES
Wdr12	WD repeat domain 12	−1.58	ES	Cort	Cortistatin	5.83	ES
Lias	Lipoic acid synthetase	−1.56	ES	Zfp324	Zinc finger protein 324	5.63	ES
				Olig2	Oligodendrocyte transcription factor 2	6.49	ES
				Dnm2	Dynamin 2	3.88	Neuron
				Gm11974	Predicted gene 11974	3.83	Neuron

Abbreviation: ES, embryonic stem.

signaling pathways (*Gnai3*, *Pick1*, and *Plce1*); and genes that play a role in membrane fusion (*Dnm2*). The wide variety of functions represented by the targets indicates that we identified targets that affect all stages of viral infection. While gene ontology enrichment analysis (See Materials and Methods) defines some pathways that would be anticipated, such as induction of apoptosis (GO: 0006917) and G-protein coupled receptor binding (GO:0001664), other unanticipated pathways such as perinuclear region of cytoplasm (GO:0048471) and ubiquitin-specific protease/thioesterase activity (GO: 0004843 and GO:0004221) were also enriched (Table 3). Interestingly, none of the nine genes previously associated with viral infection are represented by the GO term "response to virus" (GO:0009615), explaining why we did not enrich for this GO term.

Comparison of hits identified between assays and cell types indicates that, while there is overlap between time points within a given differentiation state, there is no overlap of hits between differentiation states. For example, 20 of the neuron clones overlap multiple time points, especially at 48 and 72 hours, such as *Rab5b*. Three undifferentiated clones overlap multiple time points including *Dtx3*, *Unc13d*, and *Rcor2*. Potentially, this difference is due to the replication of pluripotent cells; as neurons are postmitotic. Furthermore, the shedding hits, such as *Cort*, do not overlap with other time course assays; arguing for the specificity between the two assays. Finally, there is no overlap of targets between cell types, possibly due to differences in gene expression based on developmental stage.

We were able to independently validate that reduction of *Unc13d* or *Bbs4* leads to resistance to RABV. These genes work through independent pathways as reduction in *Unc13d* affects IFN-γ production as part of the innate immune response; whereas, reduction in *Bbs4* destabilizes the microtubular cytoskeleton and negatively alters dynein-directed viral transport and/or replication inside the cell. Further independent studies of each pathway would be required to confirm these hypotheses.

Unc13d is a signaling protein that works through the innate immune system. Unc13d has been shown to localize with cytotoxic granules at the immunologic synapse [42]. It is essential for the priming step of cytolytic granule secretion preceding vesicle membrane fusion. Jinx mice (*Unc13d* ENU mutants) are sensitive to infection by mouse cytomegalovirus [43, 44]. Natural killer cells and cytotoxic T lymphocytes fail to degranulate; and Jinx mice produced high levels of IFN-γ and IFN-α/IFN-β after infection. Increases in IFN-γ have repeatedly been shown to increase in vitro and in vivo resistance to RABV [10].

Bbs4 contributes to the microtubular cytoskeleton that is used for viral transport inside the cell. Bbs4 localizes to the centriolar satellites of centrosomes and functions as an adaptor of the p150(glued) subunit of the dynein transport machinery [45]. Silencing of BBS4 induces deanchoring of

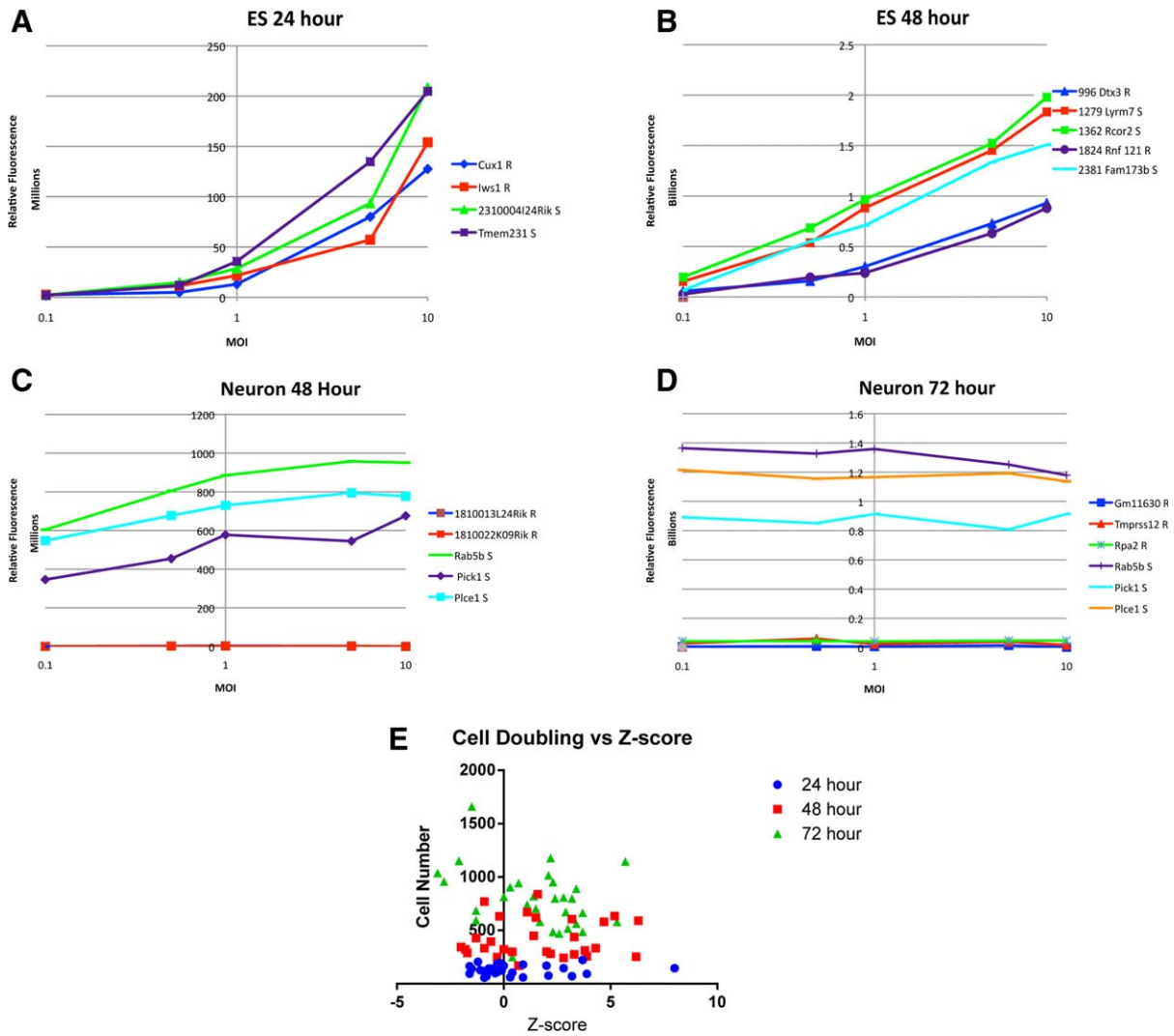

Figure 4. Secondary assays. Example dose response curves showing relative fluorescence (representative of the extent of rabies virus [RABV] infection due to green fluorescent protein-rabies) versus MOI for specific RABV hits at multiple time points **(A–D)**. Hits are named by the gene that has been disrupted. Individual graphs represent one cell type (undifferentiated ESCs or neurons) and one time point. Specific clones have been categorized as sensitive (S) or resistant (R) to RABV based on previous screening. **(E):** Depicts the lack of correlation between undifferentiated clone growth rates plotted as cell number versus *Z*-score at specific time points for RABV hits. Abbreviations: ES, embryonic stem; MOI, multiplicity of infection.

centrosomal microtubules, arrest in cell division, and apoptotic cell death. Dynein is involved in the axonal transport of RABV along microtubules through neuron cells [46]. The RABV phosphoprotein has a dynein light chain 8 (LC8) binding domain that is required for the infectivity of the virions, as it is involved in early transcription and replication in neurons [11]. Host-based dynein LC8 binds the viral phosphoprotein, and facilitates microtubule-directed minus-sense axonal transport and spread of the virus throughout the host nervous system [46, 47]. Furthermore, the capacity to bind LC8 and the binding domain are well conserved in the *Lyssavirus* genus arguing its importance for viral function [48]. Hence, targeting *Bbs4* provides a mechanism to destabilize the microtubular cytoskeleton and to negatively alter dynein-directed viral transport and/or replication inside the cell. Further research into this target could have implications for all viruses that use dynein-directed transport.

While confirmation of the two targets, *Unc13d* and *Bbs4*, through the utilization of siRNA supports the validity of the 63 hits identified in this novel screening platform, there are complications inherent to using siRNAs that may explain why other targets were not validated in this manner. The single siRNA used to target each gene may not have efficiently knocked down expression either due to inefficient transfection, lack of target specificity, or the target gene product may be so stable that it decreases too slowly for the loss-of-function phenotype to be assayed even though its mRNA is efficiently depleted. Treatment with lipofectamine can be cytotoxic, especially to neurons. Toxicity may have confounded the effects of the knockdown. More complete loss of gene function via siRNA may induce either toxicity or other unknown compensatory cell mechanisms. Finally, duration time for the knockdown of expression of targets is variable when using siRNAs. This is especially important to consider because our assays extend out at least 5 days past when siRNA was transfected into the cells. Hence, knockdowns might not be sufficiently stable to be observed at later time

Table 2. Hits with known associations with viral infection

Clone	Virus from literature	Notes	Reference	Screen phenotype	Discussion
Pick1	Coxsackie B virus	Pick1- binds coxsackie B virus (another ssRNA virus) and adenovirus receptor		Sensitive	Coxsackie B virus is a ssRNA virus
	Adenovirus	may affect cell-cell adhesion and growth	[32]		May affect cell-cell adhesion and growth
Aqr	Murine hepatitis virus	Aqr shares some sequence homology to RNA-dependent RNA polymerase of murine hepatitis virus	[33]	Resistant	Murine hepatitis virus is a ssRNA virus Loss of host RNA polymerase could affect viral transcription
Rab5	Hepatitis C	Rab5 may play a role in HCV genome replication; reduction of Rab5 expression HCV RNA synthesis	[34]	Sensitive	Loss of Rab5 appears to have differential effects for rabies and HCV
Cib1	Kaposi's Sarcoma-associated herpesvirus	CIB1 plays a role in KSHV entry and macropinocytosis and synergizes with Ephrin2A-mediated signaling	[31]	Resistant	Loss of Cib1 may result in reduced viral infection and reduced EphA2, Src, and ERK1/2 activation
Dapk1	Epstein Barr virus	cell-death serine/threonine kinase that serves as a positive mediator of apoptosis		Resistant	Loss of Dapk1 could lead to decreased apoptosis and resistance
		Dapk transfection also increases cellular response to apoptotic stimuli.	[35]		
		Dapk1 is known to be stimulated by EBV infection resulting in cell death	[36]		
Cux1	Papillomavirus	Cux1 negatively regulates Papillomavirus promoters	[37]	Resistant	Loss of Cux-1 could result in changes in viral replication
	Cytomegalovirus	binds the human cytomegalovirus promoter to repress gene expression essential for viral replication	[38]		
Fbxw7	Simian virus 40	Fbxw7/Rb1/E2f4 complex binds SV40 LT proteins	[39]	Sensitive	Loss of Fbxw7 could alter transcription of genes relevant for viral infection
Rb1	Simian virus 40	Fbxw7/Rb1/E2f4 complex binds SV40 LT proteins	[39]	Sensitive	Loss of Rb1 could alter transcription of genes relevant for viral infection
E2f4	Simian virus 40	Fbxw7/Rb1/E2f4 complex binds SV40 LT proteins	[39]	Sensitive	Loss of E2f4 could alter transcription of genes relevant for viral infection
		E2f4 may also play a role in Simian Immunodeficiency Virus encephalitis	[40]		
	Adenovirus	DNA binding protein required for transcription of the adenovirus E2A promoter			
		Mice homozygous for a knockout gene had increased susceptibility to bacterial infection	[41]		

points especially in the shedding assays and could explain why the hits that were validated using this method include those that affect early time points.

As a screening platform, utilization of a library of mutant ESCs performed well in regard to capacity for differentiation, cell type specificity, and reproducibility. First, more than 70% of the viable clones were able to differentiate into neurons. Some attrition of clones is anticipated as they have highly variable growth rates. Those with radically altered cell division rates would still be able to differentiate if allowed varied time for aggregate formation and/or differentiation. Furthermore, many genes are required for proper neuronal differentiation and maintenance. For example, *Chrna7* (*Neuronal acetylcholine receptor*) is a putative RABV receptor and has a known role in neuronal differentiation. However, despite more than five repeated attempts, *Chrna7* mutants did not reliably produce satisfactory neurons in our hands. In terms of reproducibility, the results of the secondary dose response assays support the idea that once a phenotype is defined in a certain clone, it is reproducible.

Conclusion

Overall, we demonstrated the potential for using libraries of defined stem cell mutants and high-content assays as a high-

Table 3. GO enrichment analysis of RABV hits

Assay	GO ID	Description	Total count[a]	% Main pool[a]	Height[b]	Genes	% Hits	*p*-val Fisher	*Z*-score[c]
ES 72 hours	GO:0006917	Induction of apoptosis	31	1.16	9	Sap30bp Dapk1	25	.003929	6.3
ES Shed	GO:0001664	G-protein-coupled receptor binding	9	0.34	5	Cort Usp33	18.18	.000823	10.2
Neuron 24 hours	GO:0048471	Perinuclear region of cytoplasm	51	2.8	5	Cisd Pick1 Fbxw7	37.5	.001224	5.9
Neuron 24 hours	GO:0043234	Protein complex	64	3.51	3	Cisd Pick1 Fbxw7	37.5	.0023	5.2
Neuron 48 hours	GO:0006914	Autophagy	10	0.55	5	Cisd 9430023L20Rik	8.7	.009088	5.3
Neuron 72 hours	GO:0004843	Ubiquitin-specific protease activity	4	0.22	8	Usp1 Brcc3	8.7	.002162	8.7
Neuron 72 hours	GO:0004221	Ubiquitin thiolesterase activity	5	0.27	6	Usp1 Brcc3	8.7	.003003	7.8

[a]We assessed the counts and percentages of genes matching each GO term within the main pool of genes and the subset of hits for each screen.
[b]Height gives a sense of how high (close to the root) a particular GO term is; with smaller values indicating closeness to the root. The closer to the root/beginning of the hierarchy, the more general the GO terms (e.g., molecular—function, or biological process); Height < 3 were excluded.
[c]*Z*-score based on expected versus observed counts, and a *p*-value. Sorting was based on *Z*-score; however, terms with only one match were excluded as this *Z*-score may be artificially high.
Abbreviation: GO, gene ontology.

throughput screening platform to define host-pathogen interactomes. Until now, no studies have focused specifically on host-based screens that evaluate sensitivity to RABV. Hence, this is the first screen implemented to identify host-based targets that directly affect RABV pathogenesis. This required development of novel ESC growth and differentiation protocols, high-content assays, and image analysis protocols. Sixty-three host-based genes involved in sensitivity to RABV were identified. Nine genes are known be involved in viral infection in general, but are novel to rabies infection. Two targets, Unc13d and Bbs4, were further validated using a completely independent method, siRNA. We did not exclude or disprove any of the other 61 genes that we identified. We have taken the known host factors involved in rabies infection from approximately 13 (NGFR, NCAM, CHRNA, RIG1, IRF3, STAT1, STAT2, PML, dynein LC8, eIF3h, PCBP2, FAK, and ABCE1; as discussed in Introduction) to 63. Hence, we increased the possible targets by fivefold. In comparison, when siRNA screens were completed for HIV, influenza, and West Nile, they also enriched the possible host-based targets by approximately fivefold [49]. However, siRNA screens for RABV have yet to be reported. Arguably, this study is a substantial contribution; and as a method it is extremely encouraging. These results indicate that this is a justifiable strategy and adds additional value to generation and characterization of libraries of defined stem cells as they can be used to quickly identify high impact, clinically relevant targets for development of biomarkers, diagnostics, and drugs. These protocols are relevant for screening additional Knock-out Mouse Project resources or even panels of defined patient-specific human induced pluripotent stem cells.

Acknowledgments

This work was supported by the Transformational Medical Technologies program contract HDTRA1–10-C-0063 from the Department of Defense Chemical and Biological Defense program through the Defense Threat Reduction Agency (DTRA).

Author Contributions

D.W.: conception and design, financial support, collection and/or assembly of data, data analysis and interpretation, and manuscript writing; K.L., S.G., and M.D.: conception and design, collection and/or assembly of data, and data analysis and interpretation; Q.S.: data analysis and interpretation; T.I.: conception and design, collection and/or assembly of data, data analysis and interpretation, and manuscript writing; J.C.S.: conception and design, financial support, data analysis and interpretation, manuscript writing, and final approval of manuscript.

Disclosure of Potential Conflicts of Interest

The authors indicate no potential conflicts of interest.

References

1 Consortium TIM. A mouse for all reasons. Cell 2007;128:9–13.
2 Hansen GM, Markesich DC, Burnett MB et al. Large-scale gene trapping in C57BL/6N mouse embryonic stem cells. Genome Res 2008;18:1670–1679.
3 Oakley DJ, Iyer V, Skarnes WC et al. BioMart as an integration solution for the International Knockout Mouse Consortium. Database (Oxford) 2011;2011: bar028.
4 Chew SK, Rad R, Futreal PA et al. Genetic screens using the piggyBac transposon. Methods 2011;53:366–371.
5 Wang W, Bradley A. A recessive genetic screen for host factors required for retroviral infection in a library of insertionally mutated Blm-deficient embryonic stem cells. Genome Biol 2007;8:R48.
6 Li MA, Pettitt SJ, Yusa K et al. Genome-wide forward genetic screens in mouse ES cells. Methods Enzymol 2010;477:217–242.

7 Guo G, Wang W, Bradley A. Mismatch repair genes identified using genetic screens in Blm-deficient embryonic stem cells. Nature 2004;429:891–895.
8 Schnell MJ, McGettigan JP, Wirblich C et al. The cell biology of rabies virus: Using stealth to reach the brain. Nat Rev Microbiol 2010;8:51–61.
9 Nadin-Davis SA, Fehlner-Gardiner C. Lyssaviruses: Current trends. Adv Virus Res 2008;71:207–250.
10 Rieder M, Conzelmann KK. Interferon in rabies virus infection. Adv Virus Res 2011;79: 91–114.
11 Tan GS, Preuss MA, Williams JC et al. The dynein light chain 8 binding motif of rabies virus phosphoprotein promotes efficient viral transcription. Proc Natl Acad Sci USA 2007;104:7229–7234.
12 Palusa S, Ndaluka C, Bowen RA et al. The 3' untranslated region of the rabies virus glycoprotein mRNA specifically interacts with cellular PCBP2 protein and promotes transcript stability. PLoS One 2012;7:e33561.
13 Prosniak M, Hooper DC, Dietzschold B et al. Effect of rabies virus infection on gene expression in mouse brain. Proc Natl Acad Sci USA 2001;98:2758–2763.
14 Wang ZW, Sarmento L, Wang Y et al. Attenuated rabies virus activates, while pathogenic rabies virus evades, the host innate immune responses in the central nervous system. J Virol 2005;79:12554–12565.
15 Prehaud C, Megret F, Lafage M et al. Virus infection switches TLR-3-positive human neurons to become strong producers of beta interferon. J Virol 2005;79:12893–12904.
16 Ubol S, Kasisith J, Mitmoonpitak C et al. Screening of upregulated genes in suckling mouse central nervous system during the disease stage of rabies virus infection. Microbiol Immunol 2006;50:951–959.
17 Dhingra V, Li X, Liu Y et al. Proteomic profiling reveals that rabies virus infection results in differential expression of host proteins involved in ion homeostasis and synaptic physiology in the central nervous system. J Neurovirol 2007;13:107–117.
18 Zandi F, Eslami N, Soheili M et al. Proteomics analysis of BHK-21 cells infected with a fixed strain of rabies virus. Proteomics 2009;9:2399–2407.
19 Kluge S, Rourou S, Vester D et al. Proteome analysis of virus-host cell interaction: Rabies virus replication in Vero cells in two different media. Appl Microbiol Biotechnol 2013;97:5493–5506.
20 Fouquet B, Nikolic J, Larrous F et al. The focal adhesion kinase is involved in rabies virus infection through its interaction with the viral phosphoprotein P. J Virol 2015;89: 1640–1651.
21 Ma-Lauer Y, Lei J, Hilgenfeld R et al. Virus-host interactomes—Antiviral drug discovery. Curr Opin Virol 2012;2:614–621.
22 Lingappa UF, Wu X, Macieik A et al. Host-rabies virus protein-protein interactions as druggable antiviral targets. Proc Natl Acad Sci USA 2013;110:E861–868.
23 Strubing C, Ahnert-Hilger G, Shan J et al. Differentiation of pluripotent embryonic stem cells into the neuronal lineage in vitro gives rise to mature inhibitory and excitatory neurons. Mech Dev 1995;53:275–287.
24 McNeish J, Roach M, Hambor J et al. High-throughput screening in embryonic stem cell-derived neurons identifies potentiators of alpha-amino-3-hydroxyl-5-methyl-4-isoxazolepropionate-type glutamate receptors. J Biol Chem 2010;285:17209–17217.
25 Seth RB, Sun L, Ea CK et al. Identification and characterization of MAVS, a mitochondrial antiviral signaling protein that activates NF-kappaB and IRF 3. Cell 2005;122:669–682.
26 Malo N, Hanley JA, Cerquozzi S et al. Statistical practice in high-throughput screening data analysis. Nat Biotechnol 2006;24: 167–175.
27 Bibel M, Richter J, Schrenk K et al. Differentiation of mouse embryonic stem cells into a defined neuronal lineage. Nat Neurosci 2004;7:1003–1009.
28 McNutt P, Celver J, Hamilton T et al. Embryonic stem cell-derived neurons are a novel, highly sensitive tissue culture platform for botulinum research. Biochem Biophys Res Commun 2011;405:85–90.
29 Khawplod P, Inoue K, Shoji Y et al. A novel rapid fluorescent focus inhibition test for rabies virus using a recombinant rabies virus visualizing a green fluorescent protein. J Virol Methods 2005;125:35–40.
30 Koser ML, McGettigan JP, Tan GS et al. Rabies virus nucleoprotein as a carrier for foreign antigens. Proc Natl Acad Sci USA 2004;101:9405–9410.
31 Bandyopadhyay C, Valiya-Veettil M, Dutta D et al. CIB1 synergizes with EphrinA2 to regulate Kaposi's sarcoma-associated herpesvirus macropinocytic entry in human microvascular dermal endothelial cells. PLoS Pathog 2014;10:e1003941.
32 Excoffon KJ, Hruska-Hageman A, Klotz M et al. A role for the PDZ-binding domain of the coxsackie B virus and adenovirus receptor (CAR) in cell adhesion and growth. J Cell Sci 2004;117:4401–4409.
33 Sam M, Wurst W, Kluppel M et al. Aquarius, a novel gene isolated by gene trapping with an RNA-dependent RNA polymerase motif. Dev Dyn 1998;212:304–317.
34 Stone M, Jia S, Heo WD et al. Participation of rab5, an early endosome protein, in hepatitis C virus RNA replication machinery. J Virol 2007;81:4551–4563.
35 Inbal B, Cohen O, Polak-Charcon S et al. DAP kinase links the control of apoptosis to metastasis. Nature 1997;390:180–184.
36 Lee CW, Leu SJ, Tzeng RY et al. Latent membrane protein 1 of Epstein-Barr virus regulates death-associated protein kinase 1 in lymphoblastoid cell line. Virology 2011; 413:19–25.
37 Narahari J, Fisk JC, Melendy T et al. Interactions of the cellular CCAAT displacement protein and human papillomavirus E2 protein with the viral origin of replication can regulate DNA replication. Virology 2006; 350:302–311.
38 Stern JL, Cao JZ, Xu J et al. Repression of human cytomegalovirus major immediate early gene expression by the cellular transcription factor CCAAT displacement protein. Virology 2008;378:214–225.
39 Cheng J, DeCaprio JA, Fluck MM et al. Cellular transformation by Simian Virus 40 and Murine Polyoma Virus T antigens. Semin Cancer Biol 2009;19:218–228.
40 Morgan KL, Chalovich EM, Strachan GD et al. E2F4 expression patterns in SIV encephalitis. Neurosci Lett 2005;382:259–264.
41 Rempel RE, Saenz-Robles MT, Storms R et al. Loss of E2F4 activity leads to abnormal development of multiple cellular lineages. Mol Cell 2000;6:293–306.
42 Feldmann J, Callebaut I, Raposo G et al. Munc13-4 is essential for cytolytic granules fusion and is mutated in a form of familial hemophagocytic lymphohistiocytosis (FHL3). Cell 2003;115:461–473.
43 Mesngon M, McNutt P. Alpha-latrotoxin rescues SNAP-25 from BoNT/A-mediated proteolysis in embryonic stem cell-derived neurons. Toxins (Basel) 2011;3:489–503.
44 Crozat K, Hoebe K, Ugolini S et al. Jinx, an MCMV susceptibility phenotype caused by disruption of Unc13d: A mouse model of type 3 familial hemophagocytic lymphohistiocytosis. J Exp Med 2007;204:853–863.
45 Kim JC, Badano JL, Sibold S et al. The Bardet-Biedl protein BBS4 targets cargo to the pericentriolar region and is required for microtubule anchoring and cell cycle progression. Nat Genet 2004;36:462–470.
46 Raux H, Flamand A, Blondel D. Interaction of the rabies virus P protein with the LC8 dynein light chain. J Virol 2000;74: 10212–10216.
47 Jacob Y, Badrane H, Ceccaldi PE et al. Cytoplasmic dynein LC8 interacts with lyssavirus phosphoprotein. J Virol 2000;74:10217–10222.
48 Moseley GW, Roth DM, DeJesus MA et al. Dynein light chain association sequences can facilitate nuclear protein import. Mol Biol Cell 2007;18:3204–3213.
49 Goff SP. Knockdown screens to knockout HIV-1. Cell 2008;135:417–420.


See www.StemCells.com for supporting information available online.